Available online at www.sciencedirect.com
ScienceDirect
Polymer 48 (2007) 7221–7235
polymer
www.elsevier.com/locate/polymer

Feature Article

Mechanical properties of micro- and nanocapsules: Single-capsule measurements

Andreas Fery [a,*], Richard Weinkamer [b]

[a] University of Bayreuth, Faculty of Chemistry, Department of Physical Chemistry II, Universitätsstr. 30, D95440 Bayreuth, Germany
[b] Max-Planck-Inst. for Colloids and Interfaces, Department of Biomaterials, Am Muehlenberg 1, D14424 Potsdam, Germany

Received 22 March 2007; received in revised form 17 July 2007; accepted 19 July 2007
Available online 28 July 2007

Abstract

Capsules of micron and sub-micron dimensions are abundant in nature in the form of bacterial or viral capsids and play an increasing role in modern technology for encapsulation and release of agents. The capsules' mechanical properties are of great importance in this context not only for stability but as well for transport properties in flow, rheology or adhesion. Thus, techniques that allow for single-capsule mechanical characterization have caught much attention recently and we summarize experimental developments in this field as well as theoretical background of capsule deformation with special attention to small deformation measurements. Deformation studies on polyelectrolyte multilayer capsules are introduced as a case study, since they can be tailored in their geometry and composition and are thus well-suited as a model system.

Keywords: Micromechanics; Microcapsules; AFM

1. Introduction

Research on microcapsules is a highly interdisciplinary field that benefits from contributions from various branches of natural sciences and engineering: Already in the thirties biologists, biophysicists and biochemists developed methods that allowed for studies on individual cells, launching the field of microcapsule studies. Research on biological microcapsules remains highly vital and a source of innovation nowadays but has been complemented by research on artificial microcapsule systems. Progress in material sciences allowed production of microcapsules whose structure and composition are controlled on the nanoscale [1–6]. To achieve this goal similar mechanisms to those occurring in natural systems, like supramolecular self-assembly, were exploited and most artificial microcapsule systems are to some degree biomimetic. Potential applications of such artificial systems are in most cases linked to encapsulation and release or protection of agents like medicine, fragrances, dyes or flavour additives. Microcapsules can thus be found in fields as diverse as medicine, cosmetics, food design or coating of textiles/paper to mention just a few examples. Probably the most dynamic area of artificial microcapsule development is related to drug delivery applications. Here the aim is to develop ''intelligent'' capsule systems containing medical agents that recognize and adhere to infected regions in the body and allow for targeted localized release of the medical agents in these regions only, thus limiting side effects [7–9]. Designing microcapsules for specific tasks requires understanding and controlling their physicochemical properties. Key characteristics are adhesion properties, permeability of the capsule membranes and mechanical properties. In this review we focus on the latter aspect.

Mechanical properties of microcapsules are obviously important for stability issues. In applications of both biological and artificial systems microcapsules have to provide enough robustness to avoid membrane rupture due to wear and tear. For artificial microcapsules, membrane rupture can in contrast serve as a pathway for fast and efficient release and might thus

* Corresponding author.
E-mail address: andreas.fery@uni-bayreuth.de (A. Fery).

0032-3861
doi:10.1016/j.polymer.2007.07.050

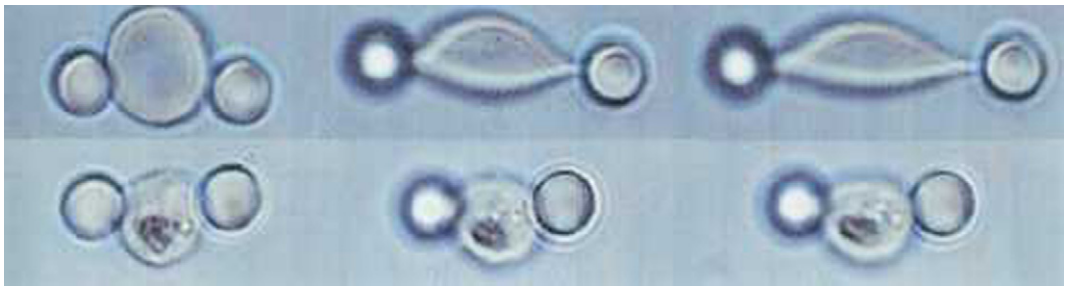

Fig. 1. Single red blood cells in a stretching experiment. Two colloidal particles are attached to the RBC and subsequently stretched by optical forces. The top row shows a healthy RBC under increasing stretching force, the bottom row a RBC which was infected by a malaria parasite. When both cells are exposed to the same forces the reduced ability of the infected cells to stretch becomes clear. Image from Ref. [13]; copyright 2004 Acta Materialia Inc.; reprinted with permission of Elsevier Sci. Ltd.

be desired under certain conditions. Stability is not ensured by simply increasing the elastic modulus of the material. Instead, microcapsules must be tailored in their complex deformation characteristics rather to efficiently perform their tasks. The great variety of mechanical properties of natural microcapsules nicely illustrates this fact [10]: red blood cells are made from membranes with the lowest bending resistance known to man but still are highly resistant against stretching [11]. This allows them squeezing through capillaries with only 10% of their diameter without any damage. These mechanical properties are vital for their biological function. For example the symptoms of malaria and sickle cell anaemia are to a large extent caused by the fact that the deformability of blood cells is changed by parasites and mutation, respectively [12]. Fig. 1 illustrates the deformation differences between malaria infected and healthy red blood cells.

Virus capsids in contrast are highly rigid with typical elastic constants similar to those of glassy polymers and can withstand pressures due to encapsulated material up to 100 atmospheres [14,15]. Apart from stability issues, mechanical properties influence the microcapsule-behaviour in an indirect fashion in many processes of interest. Microcapsule compliance for example plays an important role in adhesion: when microcapsules are adhering to surfaces a complex interplay between surface interactions, which favour establishing a contact area between capsule and surface and mechanical deformation energies, which resist capsule deformation, take place. Thus cell mechanics is well known to play a dominating role in cellular adhesion [16,17] and recent examples show that adhesion properties of artificial microcapsules can be tailored by their mechanical properties [18–22].

Another process where compliance comes into play is the transport behaviour through channels or close to adhesive surfaces [23]. Phenomena like leukocyte rolling are believed to be closely connected to the mechanical properties of the involved cells [24]. Recently, theoretical models for artificial microcapsules under rolling conditions have been introduced [25–28], which suggest novel applications for microcapsule sorting based on their mechanical properties.

While numerous techniques exist to probe the (macroscopic) rheological properties of suspensions containing capsules, there is a limited number of tools to analyse mechanical properties of micron-sized capsules on the single-capsule level. In the following, we will give a brief overview of these techniques which does not aim on completeness but rather on providing key citations and reviews for further reading. Later, the physics of capsule deformation will be discussed in more detail. In particular, the differences between measurements where large and small deformations as compared to the membrane thickness are applied will be in the center of interest here. Finally we will focus on current experimental results of small deformation measurements using the atomic force microscope and discuss perspectives of this approach.

2. Techniques for measuring microcapsule mechanics in single-capsule-experiments

Historically, the first single-capsule experiments were carried out on egg cells by Cole [29]. The cells were compressed between two parallel plates and the force was monitored as a function of the compression. From these data, the presence of an elastic cell membrane could be demonstrated and its 2D elastic modulus was estimated. Later, the setup was further refined allowing in particular shape monitoring during compression [30–36]. Fig. 2 shows a typical parallel plate-compression experiment with optical control of the shape changes during deformation and simultaneous force measurement.

The cell poking technique is a variation of this approach, where cells resting on surfaces are indented by a stylus rather than compressed by a second plate [37–39], see Refs. [40] and [41] for reviews. Similar indentation based techniques have been used for synthetic microcapsules recently [42].

The advent of the atomic force microscope has provided a tool that is ideally suited for increasing the sensitivity of indentation and plate-compression measurements to sub-micron deformations. In particular the colloidal probe AFM technique, which was independently developed by Butt [43] and Ducker [44], can be adapted such that a deformation geometry similar to a parallel plate system is achieved: The microcapsule is resting on a flat surface and compressed from above. Rather than a second flat plate, a colloidal particle of large radius of curvature is used to press onto it. The technique allows measurements of large deformations (in the order of the typical capsule dimension) or small deformations (in the order of the membrane thickness). Large deformation measurements with AFM-based setups were first carried out by Smith and

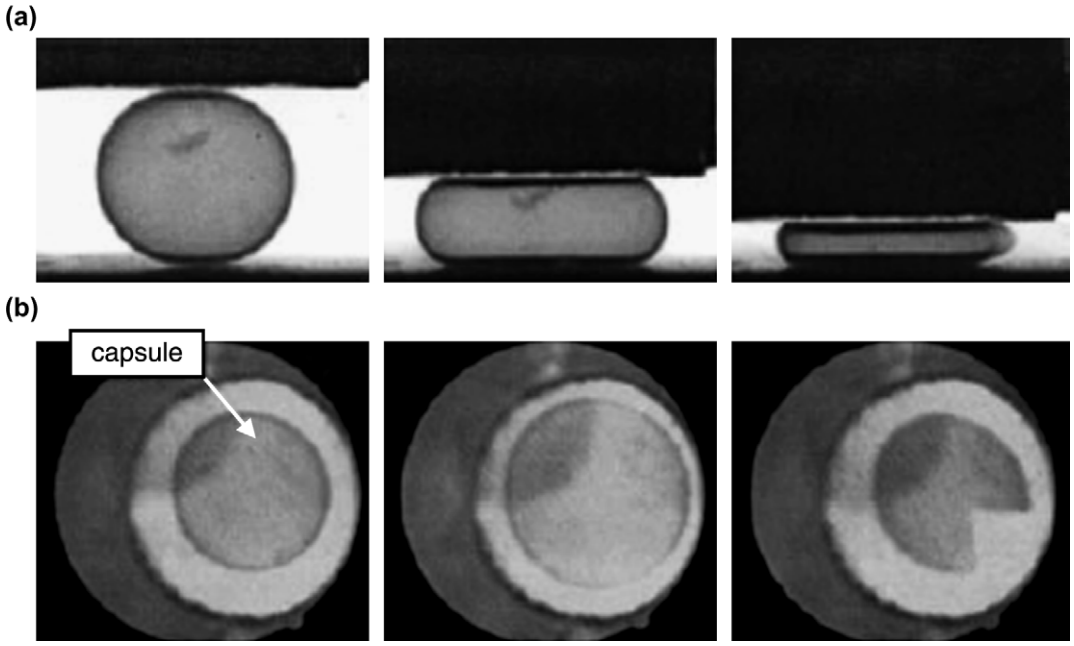

Fig. 2. Series of video images during capsule compression. Top row: side view, bottom row: top view. Images from Ref. [36]; copyright 2003 John Wiley and Sons, Inc.; reprinted with permission of Wiley-Liss, Inc., a subsidiary of John Wiley and Sons, Inc.

coworkers [45] and later by Vinogradova (see Ref. [46] and citations therein). We were the first to apply the colloidal probe method for measurements of small deformations [47] which is in many cases necessary to obtain quantitative information on material parameters like the Young's modulus. Measurements of small deformations can also be performed with sharp AFM-tips rather than colloidal probes, as it was demonstrated by various authors [48,49]. A literature overview on these cell-indentation measurements can be found in Refs. [50] and [51].

The micropipette technique was used with great success in the field of lipidic vesicles [52] and for the deformation analysis of simple cells like red blood cells [53]. A micropipette with an inner diameter of several microns is used to suck the microcapsule with a defined, hydrostatically controlled pressure. The deformation of the object is monitored with optical microscopy as a function of the applied suction pressure. From the analysis of the shape as a function of the applied pressure, the elastic properties of the membrane can be derived. In particular, bending and stretching elastic constants were measured this way. Ref. [54] can serve as a starting point for further reading.

For extremely soft membranes that show thermal shape fluctuations, mechanical properties, in particular bending elastic constants, can be derived from analysis of these fluctuations. This has been demonstrated for red blood cells and lipidic vesicles. The shapes can be monitored interferometrically (so called flicker spectroscopy) [55–57] or by phase contrast microscopy [58,59].

Recently, several methods that allow manipulating colloids with electromagnetic fields have been developed. Usually, membrane properties are probed by attaching beads to the membrane of interest and manipulating the bead [13,60–67]. Optical tweezers are most widely used for this approach [62–66], a review on applications in biology can be found in Ref. [68], recent biomedical applications are highlighted in Ref. [12]. Magnetic tweezers have as well been successfully applied [61]. Recently also setups where cells are directly stretched by light have been presented [69–71]. Typically the forces that can be achieved are in the range 1 pN ($=10^{-12}$ N) to several 100 pN, which makes these methods an attractive complementary tools for the AFM related techniques or the micropipette, where higher forces are applied.

For rather large microcapsules, elastic constants can be derived by monitoring shape changes in flow by optical microscopy. Chang and Olbricht probed capsule deformations in shear flow [72] for synthetic microcapsules. Shear flow causes elongation of the microcapsules and thus membrane stretching, which can be quantified if the shear rates are known. More recent experiments are reported in Refs. [73] and [74]. An unexpected observation is the occurrence of membrane wrinkling in shear flow (Fig. 3) [75]. This phenomenon was recently explained quantitatively and can serve as an alternate route towards estimating elastic constants [76,77]. A method that is as well limited to rather large microcapsules that are filled with materials which differ in density from the environment is the use of spinning drop rheometers [78]. Here centrifugal forces cause an oblate deformation of the rotating microcapsule. A more thorough overview over methods exploiting flow/inertia effects can be found in Ref. [79].

3. Theory of capsule deformation

Hollow, thin walled capsules are examples of curved structures with a very small extension in one spatial dimension. Such curved surface structures are generally termed shells and their mechanical behaviour is studied by shell theory [23,80–82]. The reason for the widespread use of shells in nature and technology is that the curvature of the structure allows

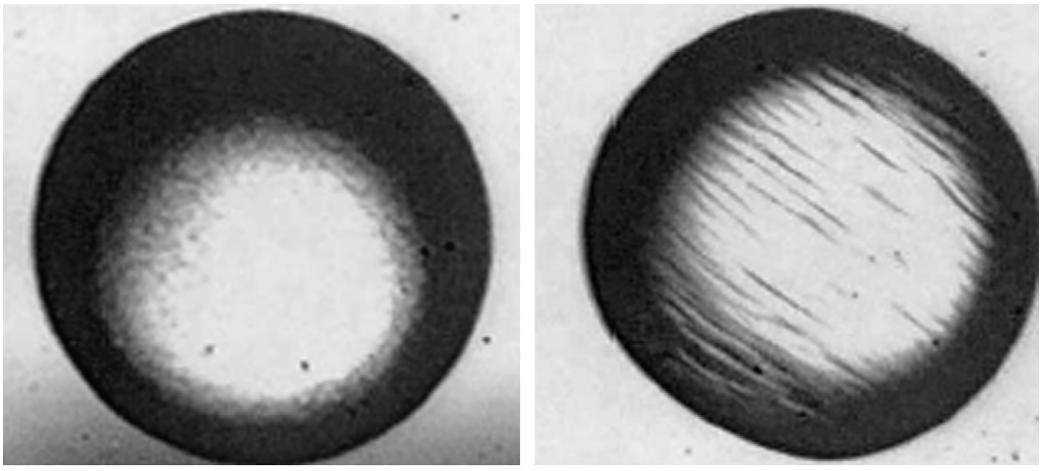

Fig. 3. An artificial microcapsule before and during deformation in shear flow. Shear causes wrinkling of the membrane with a characteristic wrinkle periodicity, which can be used for measuring the membrane's elastic properties. Image from Ref. [75]; copyright 2001 Elsevier Science B.V.; reprinted with permission of Elsevier Sci. Ltd.

a mechanical efficient use of the material by carrying transversal loading mainly by in-plane action. The main theoretical approach is to consider the wall material as a continuum. As a consequence no absolute length scale enters the theoretical description. The theory is therefore the same in describing the mechanics of e.g., microcontainers or domes of European cathedrals. The results obtained from structural engineers looking for efficient light-weight structures [83] can therefore be transformed to applications in chemistry and biology.

An important simplification is based on the fact that the thickness of the structure is much smaller than the other two dimensions. This allows a "dimensional reduction" of the problem describing the shell by its two-dimensional middle-surface. Once the two-dimensional problem is solved, the classical Kirchhoff–Love assumptions allow the "extension" in the third dimension: points on the same normal to the undeformed middle-surface stay on the same normal also after deformation, and the displacements are the same for all points at the same normal, i.e., shear deformation across the shell wall is neglected [82].

The deformation of the shell is either an in-plane stretching and shear or an out-of-plane bending. Depending on which of these deformation modes are most important and are allowed, different theories have been developed with specific applications. The characteristic of biological membranes is their low resistance to bending and shearing so that they deform either in pure bending or in-plane shear. The *shape* can be predicted by minimization of a Helfrich-type Hamiltonian [84], which includes the mean and Gaussian curvature to describe the local geometry of the membrane and the bending rigidity k and the Gaussian curvature modulus as material parameters [85,86]. The low value for k, e.g., $\kappa \approx 10^{-19}\ J \approx 10 - 20\ k_B T$ at ambient temperatures [17] gives rise to thermally activated shape fluctuations of the membrane in order to increase their configurational entropy [87]. In engineering a "membrane" is defined by being incapable of conveying moments. A membrane is therefore the two-dimensional analogue of a flexible string with the exception that it can resist compression. The in-plane membrane stresses can be determined by the condition of mechanical equilibrium only (see below), i.e., they are statically determined. The results of membrane theory therefore apply to all shells independent of the material they are made of. The general theory of shells [82], whose main ideas are outlined below and whose results for the case of a sphere which will be discussed afterwards, includes the effects of both, stretching and bending.

The mechanical problem of shell deformation can be summarized in the following set of equations [82]:

(i) kinematic equations which relate the displacement vector of each point of the middle-surface with the strain tensor (describing the in-plane stretching) and the bending tensor (describing the out-of-plane deformation);
(ii) the equations of mechanical equilibrium for the effective membrane stress tensor and the effective moment tensor;
(iii) the constitutive equations characterizing the material in relating stress and strain state;
(iv) force or displacement boundary conditions which specify the actual loading of the shell.

To exploit the two-dimensionality of the problem it is advantageous to use curvilinear coordinates instead of Cartesian coordinates to formulate the kinematic equations (i). The disadvantage of this choice is that basic results of differential geometry have to be employed. Effective stress tensors are used in the formulation of (ii) to ensure their symmetry [82]. Assuming in (iii) a material that obeys Hooke's law and that is isotropic, i.e., characterized by two material constants like Young's modulus E and Poisson ratio n, for thin shells the strain tensor is only related to the effective membrane stress tensor and the bending tensor only to the effective moment tensor. Proportionality constants are two characteristic

quantities, the extensional stiffness (1) and the bending stiffness (2).

$$\eta = \frac{Eh}{1-\nu^2} \tag{1}$$

$$\kappa = \frac{Eh^3}{12(1-\nu^2)} \tag{2}$$

Note that the thickness of the shell, h, which is assumed to be small, enters with different exponents in the mechanical parameters characterizing the ability of the shell to resist stretching and bending. The η has the dimension of an energy per area, and the contribution to the energy is calculated by a multiplication of η with the strain squared followed by an integration over the whole surface. Assuming the very simple case of a homogeneous expansion of a sphere by displacing all the points by d [88], the corresponding strain would be d/R and the stretching energy per area would therefore be given by Eq. (3).

$$E_{\text{stretch}} \propto \eta \left(\frac{d}{R}\right)^2 \tag{3}$$

The bending stiffness κ already has the dimension of energy. The bending energy is calculated by multiplication of κ by the square of the change in curvature followed again by an integration over the surface. The change in curvature is proportional to d/R^2, therefore the energy of pure bending per area can be estimated by Eq. (4).

$$E_{\text{bend}} \propto \kappa \left(\frac{d}{R^2}\right)^2 \tag{4}$$

The ratio between the two energy contributions Eq. (5) [88],

$$\frac{E_{\text{stretch}}}{E_{\text{bend}}} \propto \left(\frac{R}{h}\right)^2 \tag{5}$$

is consequently quite large for thin shells. When the shell allows a deformation without stretching, this deformation mode will be realized being energetically favourable, a statement also referred to as Love's principle of applicable surfaces. A well known result, however, is that for spherical capsules deformation modes without stretching are not possible.

In classical shell theory analytical solutions can be obtained only for simple shell geometry and simple loading conditions. In our context an important analytical result is the deformation of a spherical shell under point loads on its poles [82,89]. Close to the pole the solution turned out to be equivalent to the simple result found for shallow spheres by Reissner [90,91]. The normal displacement of the pole, d, under point loading with force P is given by Eq. (6).

$$d = \frac{\sqrt{3(1-\nu^2)}}{4}\frac{PR}{Eh^2}. \tag{6}$$

Assuming a value for the Poisson ratio $\nu = \frac{1}{3}$, we obtain the numerical prefactor and thus Eq. (7).

$$d = 0.40825\frac{PR}{Eh^2} \tag{7}$$

Away from the pole the analytical solution corresponds to the membrane solution [89], showing that the bending is limited to a restricted area around the concentrated force. An estimation of how local this bending is as a function of capsule geometry can be obtained by a simple energy argument: the linear dimension of the bent area, denoted by a, is determined by the requirement that the sum of stretching and bending energies attains a minimum (note that the bending contribution is proportional to $\kappa\frac{d^2}{a^4}a^2$, where the last factor comes from the integration over the bent area). For the spatial limitation of bending one obtains [88]

$$a \propto \sqrt{hR},$$

which means that a reduction of the shell thickness results in even more local deformation by bending.

To employ the analytical results of shell theory one has to be aware of the underlying assumptions and the limitations following from them. Most important is that the validity of Eq. (6) is restricted to small deformations, an assumption referred to as small-perturbation hypothesis [92]. This hypothesis implicates the tremendous simplification that the equilibrium conditions are not formulated in the deformed state, which is unknown and has to be determined, but in the known undeformed state, i.e. the initial spherical shape of the capsule. For thin shells deformations can be considered "small" when they are about the thickness of the shell wall. In the design of experimental procedures, which make use of analytical results in their interpretation, attention has to be paid to restrict the capsule deformation to the region of small deformations and measure within this region as accurate as possible (see following sections). For a dimensional reduction to a surface problem, the shell has to be assumed "thin". Classical thin shell theory is applicable as long as the ratio between wall thickness and shell radius is smaller than $1/10$ [93]. Considering a wall thickness of 25 nm, the capsule radius should be larger than 0.25 μm, which is doubtlessly fulfilled for the capsule systems discussed below. For the material a linear relation between stress and strain was assumed. Non-Hookean models like a Neo-Hookean model or more general a Mooney-Rivlin model have to be used to describe rubber-like materials, specifically at larger deformations [94,95].

The large deformation behaviour of spherical shells under a point load is dominated by buckling, i.e., the formation of a region of reversed curvature [96–98], which grows with increasing deformation. This type of deformation minimizes the stretching of the shell (Fig. 4).

Under the assumption that the deformation energy is localized on the rim of the formed dimple [100], Pogorelov obtained the following result Eq. (8) for the deformation under a point load P [101].

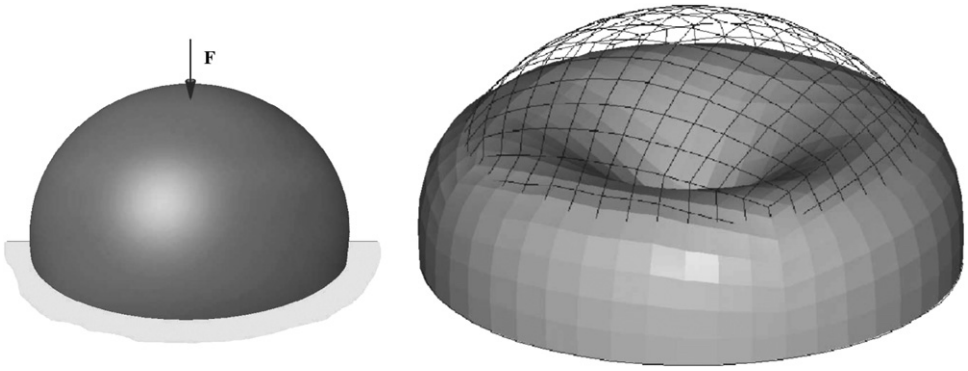

Fig. 4. Deformation of a spherical shell under a point load (loading situation prior to deformation as indicated on left hand side scheme). The shell reacts with a buckling instability for forces above a critical force. Image from Ref. [99]; copyright 2001 Elsevier Science B.V.; reprinted with permission of Elsevier Sci. Ltd.

$$d = \frac{(1-\nu^2)^2}{3.56}\frac{P^2R^2}{E^2h^5}. \quad (8)$$

In contrast to Reissners' solution for very small deformations Eq. (6) after buckling and formation of a dimple the deformation is no longer linear with the force, but quadratic.

An important extension of the spherical shell model, in particular for biological applications, is to consider that the capsule is not empty, but filled with fluid. To be more precise, a filled shell with vanishing permeability of the shell material is assumed. Evidently, the case of an empty shell is equivalent to a filled shell for a wall material of infinite permeability when inertia effects are neglected, while a finite permeability causes complex deformation-rate dependent effects. The incompressibility of the fluid inside the shell requires volume conservation at all times during deformations. For a point load force significant contributions to the potential energy arise from edge bending around the rim of the dimple, stretching due to the increase of fluid pressure inside the capsule, and the work of the applied load [102]. Fig. 5 shows a comparison between experiments performed with a racquetball ($h/R = 0.167$, thick shell!), both empty and filled with water, and analytical calculations based on axisymmetric thin shell theory. For empty shells the deformation of the shell is accurately predicted for deformations of 25% of the radius, before shear deformation, which is neglected in thin shell theory, lead to a softening of the real shell. The filling of the shell does not cause any difference for deformations up to 20% of the radius in comparison with an empty shell. This region is therefore governed mainly by bending. The effect of the displaced fluid becomes significant only for even larger deformations. An interesting behaviour of the shell stiffness as a function of shell geometry, h/R, was predicted. For a shell with a given thickness h, the shell stiffness increases with decreasing shell radius in the small deformation regime. At larger deflections, the strains are actually smaller for larger spheres. But since the strained area is proportional to R^2, the combination of both effects results in a larger shell to be stiffer than the smaller one [102].

Often biological cells are not just filled with fluid, but the fluid is under increased osmotic pressure, the so called turgor pressure. Laplace's relation gives the connection between pressure p, and the surface tension s, $\sigma \propto pR$. Starting from the general expression of the shape energy of a membrane with bending rigidity [103], an extended plate-equation was formulated and solved to describe the deformation within a confined region of cut-off radius a [104–106]. Depending on the dimensionless expression $\xi = \sigma a^2/\kappa$, a bending-dominated ($\xi \ll 1$) or a tension-dominated regime ($\xi \gg 1$) have to be distinguished [107]. The calculations took into account the finite radius of the indenter tip.

Real experimental loading conditions may deviate from the theoretical point load force scenario. Two important cases are the compression between two parallel plates and the exposure to external or internal isotropic pressure. In case of the parallel plates, an approximate analytical solution can be obtained by separating the deformation into the regions of plate-membrane contact and the non-contact regions [94,95]. Also under

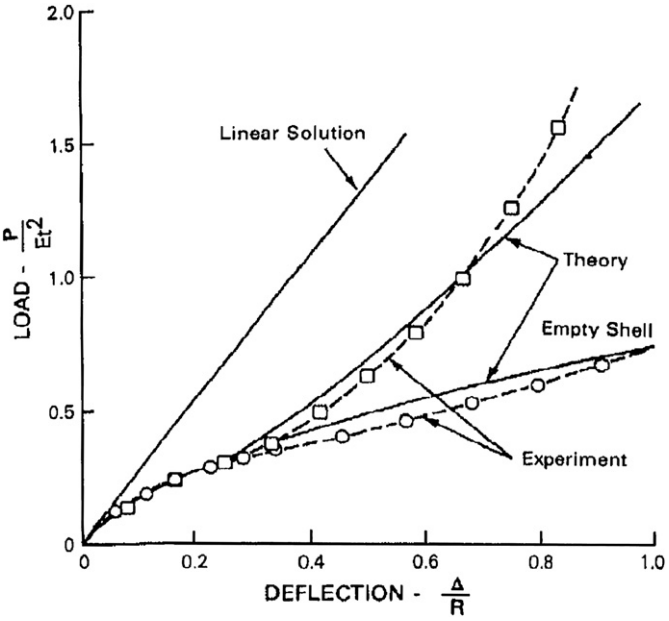

Fig. 5. Load-deflection for a racquetball with $h/R = 0.167$ (experiment) compared with calculations based on thin shell theory. The experiments were performed with empty shells (circles) and water filled shells (squares). Image from Ref. [102]; copyright 1982 American Society of Mechanical Engineers; reprinted with permission of ASME International.

isotropic external pressure buckling of the spherical shell occurs. Under the assumption that the empty shell loses stability when the work done by the external pressure equals the deformation energy, the critical pressure, p_c, for the onset of buckling is given by Eq. (9) [101,108].

$$p_c = \frac{2E}{\sqrt{3(1-\nu^2)}} \frac{h^2}{R^2}. \quad (9)$$

Based on the assumption that the deformation is concentrated at the rim of a dimple, predictions can be obtained whether the shell displays one large dimple, or several smaller ones [109]. The case of swelling of the capsule due to an internal osmotic pressure is discussed in Ref. [46]. Additional forces can act on the capsule from its interaction with a substrate. The problem of adhesion and deformation under adhesion [110,111] is of technological importance.

For a detailed analysis of large deformation of capsules with a general loading geometry numerical methods have to be employed. The loss of stability at the onset of buckling also remains a challenging problem for numerical methods. Two main numerical methods are used, on the one hand finite element modelling, a standard numerical tool for engineers, and on the other, elastic networks of triangulated surfaces, a model preferentially used in the physics community. The finite element method (FEM) is efficient in finding approximate solutions for the partial differential equations of continuum mechanics in complex geometry. The method is well documented in several textbooks [112–114], and commercial software packages are available. A finite element analysis of the deformation behaviour of spherical shells in the context of hollow sphere metal foams can be found in [115]. Using FEM the experimental conditions of a colloidal probe AFM force spectroscopy measurement was modelled. A polyelectrolyte microcapsule was compressed not by a point force but by a rigid sphere of large radius compared to the capsule radius. The calculations showed that the solution of Reissner Eq. (6) is also applicable for this loading geometry, even over a deformation range given by a few multiples of the shell thickness [116]. To reduce the computational effort, symmetries of the solution are often assumed, e.g., in the case of axisymmetric loading the solution also should display this symmetry. Evidently this excludes the description of deformation states characterized by symmetry breaking (see Fig. 6).

Although in FE calculations the geometry is discretized in ‘‘finite elements’’, results should be independent of the chosen discretization. This is routinely tested using different mesh sizes. A similar argument holds for triangulated network models, where an increase in the number of triangles renders a more accurate description of a spherical capsule. Especially appropriate and therefore employed are network models in simulations of systems which exhibit by design a discretized

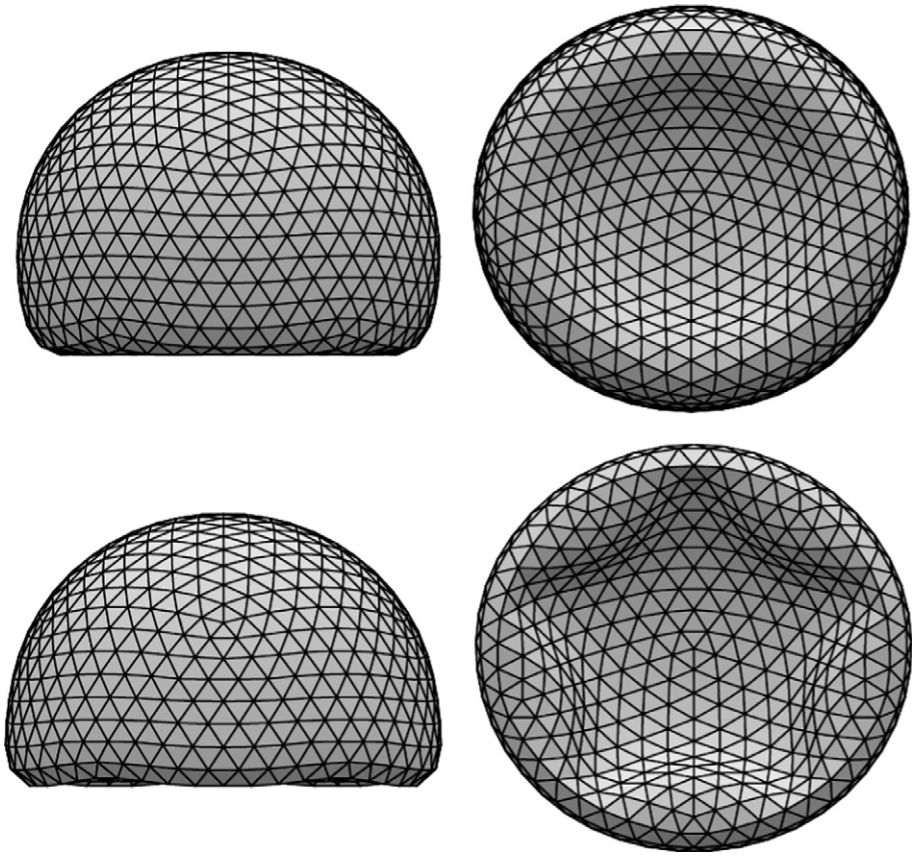

Fig. 6. While deformations of buckled shells start axisymmetrically, for larger deformations this symmetry is broken. The figure displays side and bottom views of the same shell before and after symmetry breaking. Image from Ref. [110]; copyright 2005 EDP Sciences, Società Italiana di Fisica, Springer-Verlag; reprinted with permission of EDP Sciences.

geometry. Wonderful examples from nature are virus capsids and crystalline surfactant vesicles. The structure of most virus capsids corresponds to triangulated icosahedra consisting of pentavalent and hexavalent morphological units and therefore resembling in its topology fullerene molecules, like that displayed in Fig. 7.

In network models the vertices – corresponding to viral capsomers – are connected by harmonic springs with spring constant k and equilibrium distance r_0. The total energy includes contributions from stretching and bending and is given by Refs. [117–119]

$$H = \frac{k}{2}\sum_{<i,j>}\left(|r_i - r_j| - r_0\right)^2 + \frac{g}{2}\sum_{<I,J>}\left(n_I - n_J\right)^2,$$

where sums extend over the nearest neighbour vertices (triangular surfaces) i and j (I and J) and $\boldsymbol{n}_I$ denotes the normal vector of a triangular surface. The parameters k and g are related to the two-dimensional Young's modulus, Y, and the bending rigidity, κ, via $Y = 2k/\sqrt{3}$ and $\kappa = \sqrt{3}g/2$, respectively. An important dimensionless parameter, characterizing the mechanics of the capsule as a ratio between stretching and bending contributions, is the Föppl–von Kármán number $\gamma = YR^2/\kappa$, R again the radius of the capsule. It was demonstrated that the value of γ determines the equilibrium shape of the triangulated shell. For roughly $\gamma < 130$ the shells display a rounded shape, whereas for larger values of γ, the pentavalent units in the structure become unstable leading to a faceting of the shell [118]. Based on these results it was hypothesized that shape changes observed in viral capsids can have their reason in changes of the Föppl–von Kármán number. Using elastic network models the mechanical properties of shells of icosahedral symmetry under uniaxial compressive load applied by a sphere were studied. Depending on γ, in the simulations two globally different force–deformation scenarios have been observed. For small γ a linear dependence of the force on the deformation was found. For larger values of γ the shell undergoes a buckling transition. Whereas large shells could be well described by classic continuum shell theory, small shells of the size of typical viral capsids behaved differently already for small deformations [119]. The approach of triangulated networks and studies of their buckling transitions have been applied to capsids with non-icosahedral symmetries [120], for shells under the constraint of volume conservation [117] and in connection with adhesion to a substrate [110]. In all these cases mechanical energy is assumed to dominate over thermal contributions. In the case of very soft shells thermal shape fluctuations have to be taken into account (see, e.g., Ref. [121]).

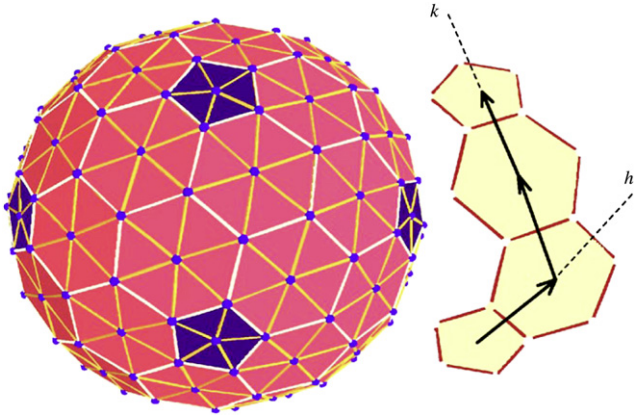

Fig. 7. Triangulated network model with pentavalent (blue) and hexavalent elements idealizing a virus structure. The plot aside demonstrates the Caspar–Klug classification of poligonalised spheres: two non-negative integers (h and k) describe the minimum number of translations on two distinct spherical geodesics to arrive from one pentavalent element at a neighbouring one ($h = 1$ and $k = 2$ in the depicted case). Image from Ref. [117] (for interpretation of the references to colour in this figure legend, the reader is referred to the web version of this article); copyright 2006 American Physical Society; reprinted with permission of the American Physical Society.

4. Small deformation measurements: experimental results

Small deformation experiments on microcapsules are of particular interest for microcapsule characterization for two main reasons. First, in large deformation experiments, the larger strains to which the microcapsules are exposed to can cause irreversible deformations for plastic materials. Thus large deformation experiments are in this case often destructive while in small deformation experiments, strains below the plasticity limit can be used, allowing for non-destructive measurements. Second, in large deformation experiments, the (changes or conservation) of the internal microcapsule volume plays an important role. While this is not a problem for strictly impermeable membranes, often microcapsule membranes are found to show finite permeability for the encapsulated medium/solvent on the timescale of the experiment. In this case, the internal volume change has to be taken into account to derive the membrane properties from the experiment. This requires assumptions on the permeability which are not straight forward and difficult to check with independent methods, especially if permeability of small molecules like water is concerned. In contrast, volume changes are higher order effects in small deformation measurements and no assumptions on permeability are necessary.

As mentioned above, no absolute length scale enters the theoretical description of shell deformation, and indeed for testing mechanical models, experiments on macroscopic objects are well-suited. One example is experiment on the compression of ping pong balls carried out by Pauchard (Fig. 8) [122,123], where the material constants are well known and comparison with shell theory can be made.

To perform small deformation experiments, independently of the shell size, deformations in the order of the shells' wall thickness have to be applied. If microcapsules are the subject of investigation nanometer control of the deformation is necessary, as typical wall thicknesses are between 1 and 100 nm. This poses enormous technical requirements, which have only been met by recent technological developments.

Optical tweezers were first used for microcapsule deformation measurements that could be quantitatively interpreted in terms of elastic constants. Helfer and coworkers investigated the deformation of actin coated vesicles and found clear signatures of a buckling instability [63–65].

Fig. 8. Ping pong balls are good macroscopic examples for shells as they display the main features of shell deformation (linear elastic response at deformations in the order of the wall thickness followed by buckling instabilities at larger deformations). Image courtesy S. Komura, (Tokyo Metropolitan Univ, Fac Sci, Dept Chem, Tokyo 1920397, Japan).

The most widely used device for small deformation measurements is the atomic force microscope (AFM), which will be in focus in the following. It provides a broader dynamic force range between several 10^{-12} N and 10^{-6} N combined with deformation resolutions better than 1 nm. In order to probe elastic constants of microcapsules with an AFM, the microcapsules have to be immobilized on a solid support. Subsequently, a force–deformation measurement is performed, during which the AFM-probe exerts a known force on the pole of the microcapsule while the deformation is monitored. The force is measured by monitoring the deflection of the AFM-cantilever, after suitable calibration of the cantilever's spring constant [124,125]. The deformation can only be inferred indirectly; by reference measurements on non-deformable surfaces (usually the substrate is used as a reference).

For a part of the measurements reported in the following, instead of a sharp AFM tip, a colloidal probe AFM setup was used. In the colloidal probe method, that was developed earlier by Butt [43] and Ducker [44], a colloidal particle of diameter of several microns is glued to a tipless AFM-cantilever and used as a probe. The main reason for the use of the colloidal probe technique is that the geometry of the contact between capsule and cantilever is well defined and that high stresses on the microcapsule as they arise for sharp AFM-tips are avoided.

5. Case study: polyelectrolyte multilayer capsules

Polyelectrolyte multilayer capsules (PMCs) are well-suited as a model system to study the characteristics of microcapsule deformation and demonstrate at the same time the advantages of the small deformation approach. Therefore we will report on recent experiments on this system in the following in more detail before giving an overview on other experiments using the small deformation approach.

PMCs are formed by template-assisted self-assembly on solid particles. The microcapsule production process here is based on the layer-by-layer self-assembly [lbl-sa], which was first introduced by Decher and coworkers as a surface coating technique [126,127]. Polyelectrolyte multilayers can be built up on charged surfaces by alternating adsorption of positively and negatively charged polyelectrolytes from aqueous solution. For many polyelectrolyte combinations, the total thickness of the surface coating is linear in the number of deposition cycles, with a thickness increase per polyelectrolyte layer pair in the order of nanometers. The thickness of the layer is thus very well defined and tunable. Hollow capsules can be produced by a two-step process [128]. First colloidal particles are coated using lbl-sa, then the core particles are dissolved under conditions that do not destroy the multilayer shell. Composition and thickness of the shell walls can be controlled with a precision that is comparable with the case of solid-supported lbl-esa films. Additionally, the capsules have the same shape and monodispersity as the template particles. This makes them one of the best-defined capsule systems with respect to these parameters that are currently available (Fig. 9). While due to the stepwise deposition process, one would intuitively expect a laminated structure of the layers, for the majority of polyelectrolyte multilayers a strong interdigitation is found and the wall material can therefore be treated as homogeneous [126]. Recent reviews on the subject can be found in Refs. [3,4]. In the following we will discuss deformation experiments of PMCs from polyallylamine and polystyrene-sulfonate (PAH/PSS) in water, which is the most widely used system.

Concerning the deformation properties, this system poses severe problems for large deformation measurements. The PAH/PSS capsule system was previously studied by two

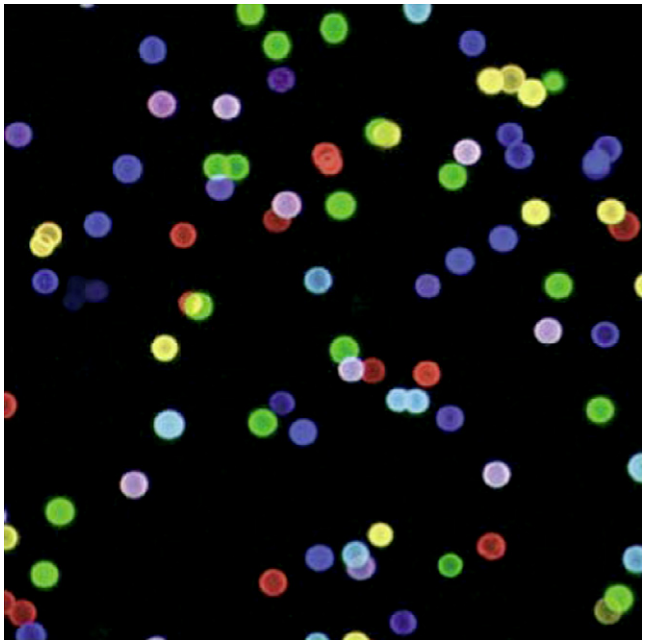

Fig. 9. Polyelectrolyte multilayer capsules offer well defined radius and wall thickness, combined with broad versatility of composition. Here, multiple fluorescent labels were integrated in the wall, which could allow for recognition and tracking of capsules in flow cytometry. Image from Ref. [4]; copyright 2003 Capsulution Nanoscience AG; reprinted with permission of Capsulution Nanoscience AG.

groups. Bäumler and coworkers used micropipette sucking [129] and found that these microcapsules show, unlike for example lipid vesicles, no shape changes up to a critical pressure. After the critical pressure, irreversible collapse of the capsules was observed. Gao [108,130] used osmotic pressure to trigger capsule collapse and could successfully describe the collapse as a buckling transition. In both cases, deformation experiments were thus destructive and irreversible.

The capsules show no mechanism that ensures volume conservation, which would have suppressed the buckling transition. Volume exchange between inside and outside happens on a timescale in the order of seconds. Permeability of the capsule membrane for water seems to be rather large. Permeability plays an important role for large deformation measurements, which we have discussed in detail in Ref. [131]: for an impermeable capsule, the dominating term in the deformation energy stems in this case from the stretching of the capsule membrane which occurs due to conservation of the encapsulated volume. For a permeable capsule, this conservation is only partial and depends on the permeability of the membrane. Thus, the capsule stiffness mainly reflects the permeability properties on the timescale of the experiment, and not the membrane's mechanical properties. Both the plasticity and the permeability problem can be overcome using the small deformation approach as explained in the following.

Fig. 10 shows a typical force–deformation relation of an individual microcapsule in water. The microcapsule presents a linear force–deformation relation for deformations in the order of the capsule wall thickness as well as a rather complex deformation behaviour including step-like instabilities for larger deformations.

In order to understand the reason for the instabilities in the deformation behaviour, a combination of colloidal probe AFM with reflection interference contrast microscopy (RICM) turns out to be useful. The AFM setup is installed on top of an inverted optical microscope. In this way, it is possible to monitor the contact zone between the colloidal probe and the (transparent) substrate with reflection interference contrast microscopy [132,133]. Fig. 11 shows a schematic of the setup, further experimental details can be found in Ref. [47].

Thus shape changes can be correlated with the forces acting on the shell. Using this approach, it can be shown that the instabilities at larger deformations correlate with buckling events like that displayed in Fig. 6 [47,134]. In small deformation measurements, however, such instabilities are avoided, which can be checked by the microinterferometry information. Apart from capsule shape tracking, microinterferometry can be also used to ensure symmetric capsule loading conditions.

If the experiment is limited to small deformations, a simple linear force–deformation relation is observed. The deformation is fully reversible and thousands of experiments can be carried out on the same capsule. This non-destructivity allows following dynamic processes. The linearity of the force–deformation relation is indeed expected for a membrane with non-vanishing bending stiffness. According to Reissner [90,91], the deformation d is related to the force P, the capsule radius R, the wall thickness h, the Young's modulus E and the Poisson Ratio n via Eq. (6). While this relation is strictly valid only for a point force load at the apex of a shallow spherical cap, it is also a good approximation for this loading situation (a shell compressed by a large sphere) as revealed by finite element modelling [116].

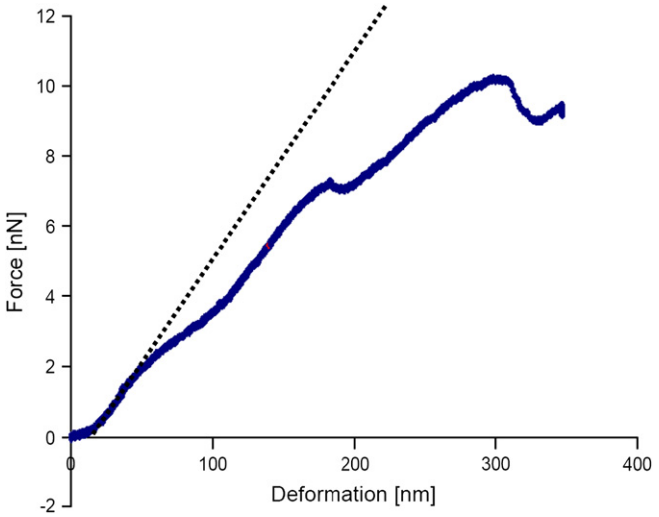

Fig. 10. Blue symbols: experimental force–deformation characteristic of a PAH/PSS capsule of 25 nm dry thickness and 7.9 μm radius in water. Dotted line: Reissner's result for deformations up to 50 nm (valid for a thin, shallow shell). (For interpretation of the references to colour in this figure legend, the reader is referred to the web version of this article.)

Because in the microcapsule system, both the capsule radius and the capsule wall thickness can be varied, the validity of the Reissner approach can be tested by checking the scaling of the capsule stiffness ($k = P/d$) with these parameters. In Fig. 12, measured k-values for capsules with different radius R and wall thickness h are compiled to form a master plot. One can clearly see, that k is indeed proportional to the square of the membrane thickness h and inversely proportional to the capsule radius R, as predicted by Reissner. This also means that surface tension or other interactions between the wall and water phase play in this case no important role since their contribution should not depend on wall thickness and would thus result in an offset of k at $h = 0$, which is within the accuracy of the measurement not detectable. Another consequence is that the mechanical properties of the wall are compatible with a homogeneous wall model. This is in fact expected, since the individual layers are strongly inter-digitated [126].

Thus, the elastic properties of the capsule wall can be determined, as all parameters except for the wall materials' Young's modulus and Poisson ratio can be measured independently. The Young's modulus of PAH/PSS capsules in pure water is found to be in the order of several hundred mega pascals [135], which is in good agreement with independent measurements on flat layers by others [136].

These experiments offer several advantages as measurements can not only be carried out in solvent, but solvent properties like salt concentration [135], pH [137] or temperature [138] can be varied during the mechanical properties' probing. Due to the non-destructive nature of the measurement, changes in mechanical properties can even be followed in situ for

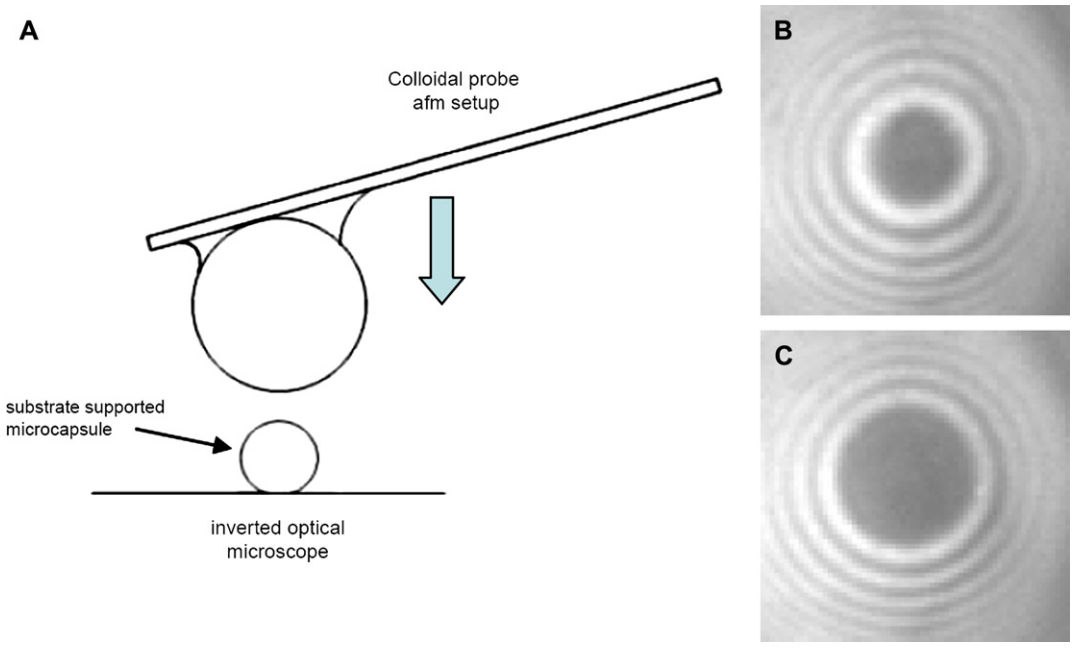

Fig. 11. A is a schematic sketch of a colloidal probe AFM setup for microcapsule compression. The microcapsule is immobilized on a flat substrate and is compressed by a large colloidal particle (the particle diameter is large as compared to the capsule), which is glued to an AFM-cantilever. The cantilever is integrated into the AFM setup. The optical microscope below allows high-resolution imaging of the contact zone. B is a typical microinterferometry image of the capsules' contact zone, C shows the same capsule under an applied load which increases the contact area.

individual capsules. The rate dependency of deformation properties merits special attention, when studying viscoelastic membranes. A nice example of such a system is shown in Fig. 13 where PMCs are probed below and above the glass transition of the wall material. In the high temperature case k is rate dependent while at room temperature no rate dependency is observed. The rate of deformation can be varied by 2–3 orders of magnitude with existing setups.

6. AFM-based small deformation experiments, an overview

The basic experimental features reported above are not specific for this particular capsule system but are, in fact, rather

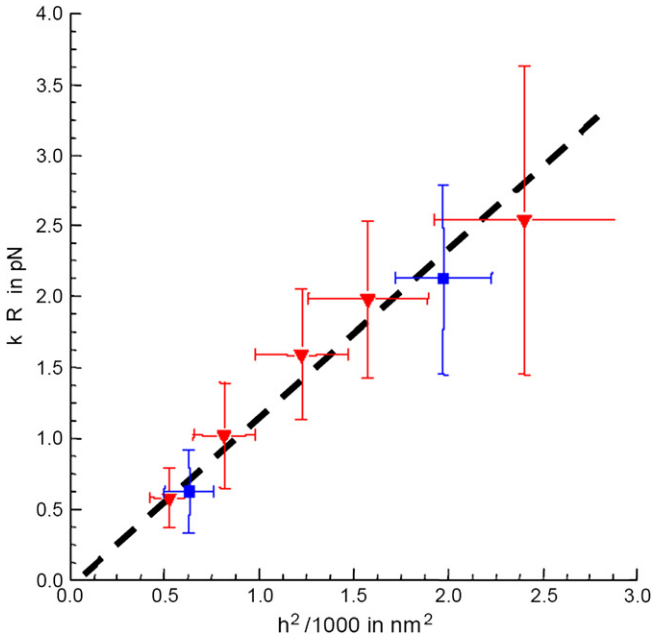

Fig. 12. Master plot for deformation experiments: the microcapsule stiffness is multiplied with the shell radius and plotted versus the square of the membrane thickness. The data from microcapsules of different radii collapses onto a master curve. Red triangles: shells with 9.6 μm radius, blue squares: shells with 7.85 μm radius. Dashed line: best linear fit (for interpretation of the references to colour in this figure legend, the reader is referred to the web version of this article).

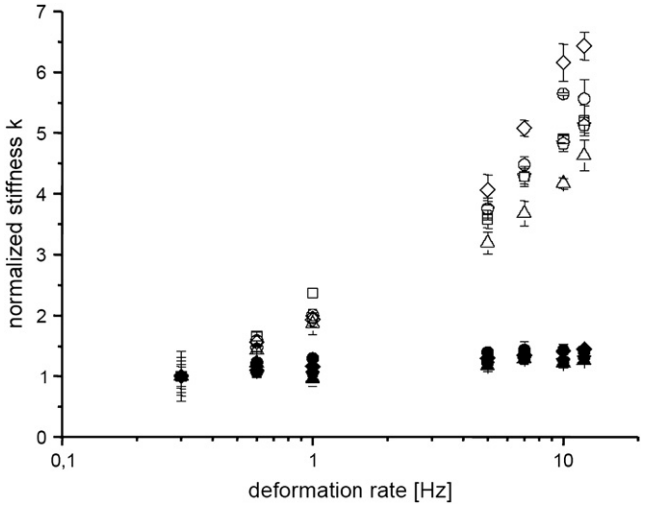

Fig. 13. Stiffness of capsules (normalized to stiffness at deformation rate 0.3 Hz) at room temperature (closed symbols) and at 70 °C (open symbols) as a function of the deformation rate (no rate dependency is observed for low temperature while a pronounced rate dependency is observed at 70 °C, indicating viscoelastic properties). Image from Ref. [138]; copyright 2005 American Chemical Society; reprinted with permission of the American Chemical Society.

universal for capsules of various compositions and dimensions and the continuum mechanical concepts hold even down to systems with nanometer thickness.

Deformation experiments on solid-supported gel state liposome-vesicles made from dipalmitoyl-phosphatidylcholine (DPPC) with radius between 50 and 200 nm show similar linear force–deformation characteristics as reported above [139]. The vesicle stiffness k scales inversely proportional to the vesicle radius R, as found for the PMCs. Elastic constants of the DPPC membrane were thus calculated and compared favourably with independent measurements [140].

In biological systems, much attention has recently been attributed to deformation measurements of individual virus capsids [15]. Using approaches analogous to the Reissner approach, elastic constants of the capsid shell were determined. Pronounced differences between empty and filled capsids [141] or young and matured viruses [142] were detected.

These measurements reveal a special feature of the virus capsids which are not strictly spherical but have a facetted structure. This can cause deviations from the Reissner deformation characteristics [117,119]. Indeed, measurements on facetted catanionic vesicles indicate that faceting causes pronounced reinforcements, which might play an important role in increasing virus stability [143].

The deformation of tubes shares many similarities with capsule deformation and several AFM-based experiments of tube-like structures have been reported recently. Tubes, like capsules, present a linear force–deformation relation followed by buckling instabilities upon compression. Similar to the capsule case, scaling laws, which nevertheless differ from the capsule case can also be derived for tubes [144]. Indeed, buckling instabilities were experimentally found for microtubules [144] and for self-assembled protein nanotubes [145,146]. Again the tubes' stiffness in the pre-buckling regime served as a measure of the wall materials' elastic constants. Recently, the scaling behaviour predicted by de Pablo and coworkers was confirmed for polyelectrolyte multilayer hollow tubes of variable radius [144,147,148].

7. Conclusion

Mechanical characterization of individual microcapsules is a field of growing importance at the border of biophysics and material sciences, combining both theoretical and experimental challenges. We gave in the first part of the paper a broad overview which aims not at depth but rather at providing first key references to the reader. In the second part, we focused on a particular novel approach, namely small deformation experiments on shell structures.

The standard theoretical approach is to employ continuum mechanics in the form of shell theory. The complexity of the partial differential equations allows analytical solutions only under strong simplifications. One important exception is when only small deformations are considered, e.g., the result of Reissner for a spherical shell under a concentrated load. Improved computational resources and algorithms facilitate a numerical treatment of shell deformation problems. Finite element models and spring network models nowadays are widely and successfully used. The consideration of defects in the shell wall material and the instabilities connected with buckling events of the shell structure remain, however, a challenge for computational models.

Experimentally, this approach has experienced a boost with the advent of novel techniques which allow for nanoscale deformation experiments. In particular the atomic force microscope has in this context been used in the past years with much success. We discussed in detail results on artificial microcapsules made from polyelectrolyte multilayers, which can serve as a model system with adjustable and well defined radius, wall thickness and composition. However, various examples from biology and materials science demonstrate the generality of the approach. The main advantages of performing small deformation experiments are that capsule deformation becomes independent of permeability properties and that non-destructive experiments can be carried out on materials with a low elastic limit. As well, microcapsules with diameters as low as 30 nm have already been probed which are inaccessible with other approaches.

Still, many new fundamental questions and experimental challenges have been raised about investigating systems of even smaller dimensions. One critical issue, where theoretical descriptions beyond purely continuum mechanics are needed, is the effect of surface tension on deformation. This effect was shown to be negligible in some cases [116], but it significantly affects deformation properties especially when the radii of curvature become smaller and large surface tensions are present [149]. For charged systems, membrane tensions can arise from (Coulomb) self-repulsion which has been found to result in swelling of microcapsules upon changes in salt concentration [150], pH [137,151–154] or temperature [150,155]. Recently, the first theoretical descriptions of these phenomena have been presented [156,157] but their impact on deformation properties is still subject of current research. Finally, many materials in nature are not homogeneous, but rather composites which pose additional challenges and perspectives in developing systems with tailored and switchable deformation properties. On the experimental side, much interest exists in expanding the deformation-rate over a broader range, as it is the case in mechanical testing of macroscopic polymeric materials. At the same time, the power of in situ optical access during deformation is just emerging and much further development is to be expected in this direction in the near future.

References

[1] Tarcha PJ. Polymers for controlled drug delivery. Boca Raton: CRC; 1991.
[2] Meier W. Chemical Society Reviews 2000;29(5):295–303.
[3] Möhwald H, Donath E, Sukhorukov G. Smart capsules. New York: Wiley VCH; 2003.
[4] Peyratout CS, Dähne L. Angewandte Chemie International Edition 2004;43:3762–83.
[5] Discher BM, Won Y-Y, Ege DS, Lee JC-M, Bates FS, Discher DE, et al. Science 1999;284:1143–6.

[6] Dinsmore AD, Hsu MF, Nikolaides MG, Marquez M, Bausch AR, Weitz DA. Science 2002;298(5595):1006–9.
[7] Langer R. Nature 1998;392(6679):5–10.
[8] Ai H, Jones SA, de Villiers MM, Lvov YM. Journal of Controlled Release 2003;86(1):59–68.
[9] Ferrari M. Nature Reviews Cancer 2005;5(3):161–71.
[10] Ananthakrishnan R, Guck J, Kas J. Recent Research Developments in Biophysics 2006;5:39–69.
[11] Lipowsky R, Sackmann E. Structure and dynamics of membranes, vol. 1A. Amsterdam: Elsevier; 1995.
[12] Suresh S. Journal of Material Research 2006;21(8):1871–7.
[13] Suresh S, Spatz J, Mills JP, Micoulet A, Dao M, Lim CT, et al. Acta Biomaterilia 2005;1:16.
[14] Zandi R, Requera D. Physical Review E 2005;72(2):021917.
[15] Ivanovska IL, Pablo PJC, Ibarra B, Sgalari G, MacKintosh FC, Carrascosa JL, et al. Proceedings of the National Academy of Sciences of the United States of America 2004;101(20):7600–5.
[16] Gumbiner BM. Cell 1996;84:345–57.
[17] Boal DH. Mechanics of the cell. Cambridge: Cambridge University Press; 2002.
[18] Seifert U, Lipowski R. Physical Review A 1990;42(8):4768–71.
[19] Elsner N, Dubreuil F, Fery A. Physical Review E 2004;69:031802.
[20] Shull KR. Materials Science and Engineering R-Reports 2002; 36(1):1–45.
[21] Graf P, Finken R, Seifert U. Langmuir 2006;22:7117–9.
[22] Schwarz U. Soft Matter 2007;3(3):263–6.
[23] Pozrikidis C. Modeling and simulation of capsules and biological cells. London, UK: CRC Press; 2003.
[24] Schwarz US, Alon R. Proceedings of the National Academy of Sciences of the United States of America 2004;101(18):6940–5.
[25] Alexeev A, Verberg R, Balazs AC. Macromolecules 2005;38: 10244–60.
[26] Alexeev A, Verberg R, Balazs AC. Soft Matter 2006;2(6):499–509.
[27] Alexeev A, Verberg R, Balazs AC. Physical Review Letters 2006;96: 148103.
[28] Smith KA, Alexeev A, Verberg R, Balazs AC. Langmuir 2006;22: 6739–42.
[29] Cole KS. Journal of Cell and Comparative Physiology 1932;1:1.
[30] Bartkowiak A, Hunkeler D. Chemistry of Materials 1999;11:2486.
[31] Edwards-Levy F, Levy MC. Biomaterials 1999;20:2069.
[32] Hiramoto Y. Experimental Cell Research 1963;32:59.
[33] Rehor A, Canaple L, TZhang Z, Hunkeler D. Journal of Biomaterials Science Polymer Edition 2001;12:157.
[34] Zhang Z, Blewett JM, Thomas CR. Journal of Biotechnology 1999; 71:17–24.
[35] Zhang Z, Saunders R, Thomas CR. Journal of Microencapsulation 1999;16:117.
[36] Carin M, Barthes-Biesel D, Edwards-Levy F, Postel C, Andrei DC. Biotechnology and Bioengineering 2003;82(2):207–12.
[37] McConnaughey WB, Petersen NO. The Review of Scientific Instruments 1980;51:575–80.
[38] Petersen NO, McConnaughey WB, Elson EL. Proceedings of the National Academy of Sciences of the United States of America 1982; 79:5327–31.
[39] Daily B, Elson EL. Biophysical Journal 1984;45:671–82.
[40] Zhalak GI, McConnaughey WB, Elson EL. Journal of Biomechanical Engineering-Transactions of the ASME 1990;112(3):283–94.
[41] Goldmann WH. Biotechnology Letters 2000;22(6):431–5.
[42] Hsu MF, Nikolaides MG, Dinsmore AD, Bausch A, Gordon VD, Chen X, et al. Langmuir 2005;21(7):2963–70.
[43] Butt HJ. Biophysical Journal 1991;60(6):1438–44.
[44] Ducker WA, Senden TJ, Pashley RM. Nature 1991;353:239.
[45] Smith AE, Zhang Z, Thomas CR, Moxham KE, Middelberg APJ. Proceedings of the National Academy of Sciences of the United States of America 2000;97(18):9871.
[46] Vinogradova OI. Journal of Physics: Condensed Matter 2004;16:1105.
[47] Dubreuil F, Elsner N, Fery A. European Physics Journal E 2003; 12(2):215–21.
[48] Shroff SG, Saner DS, Lal R. American Journal of Physiology – Cell Physiology 1995;269(1):C286–92.
[49] Radmacher M. IEEE Engineering in Medicine and Biology Magazine 1997;16:47.
[50] Radmacher M. Measuring the elastic properties of living cells by the atomic force microscope. San Diego: Elsevier Science (USA); 2002.
[51] Zelenskaya A, de Monvel JB, Pesen D, Radmacher M, Hoh JH, Ulfendahl M. Biophysical Journal 2005;88:2982.
[52] Kwok R, Evans E. Biophysical Journal 1981;35(3):637–52.
[53] Hochmuth RM, Evans E. Biophysical Journal 1982;39:71–81.
[54] Needham D, Zhelev DV. Surfactant Science Series 1996;62: 374–439.
[55] Fricke K, Withensohn K, Laxhuber R, Sackmann E. European Biophysics Journal with Biophysics Letters 1986;14(2):67–81.
[56] Brochard F, Lennon JF. Journal de Physique 1975;36(11):1035–47.
[57] Engelhardt H, Duwe HP, Sackmann E. Journal de Physique Lettres 1985; 46(8):L395–400.
[58] Meleard P, Gerbeaud C, Pott T, FernandezPuente L, Bivas I, Mitov MD, et al. Biophysical Journal 1997;72(6):2616–29.
[59] Döbereiner HG, Evans E, Kraus M, Seifert U, Wortis M. Physical Review E 1997;55:4458–74.
[60] Gittes F, Schmidt CF. Methods in Cell Biology 1998;55:129.
[61] Guttenberg Z, Bausch AR, Hu B, Bruinsma R, Moroder L, Sackmann E. Langmuir 2000;16(23):8984–93.
[62] Dimova R, Poulingny B, Dietrich C. Biophysical Journal 2000;79: 340–56.
[63] Helfer E, Harlepp S, Bourdieu L, Robert J, MacIntosh FC, Chatenay D. Physical Review Letters 2000;85(2):457–60.
[64] Helfer E, Harlepp S, Bourdieu L, Robert J, MacIntosh FC, Chatenay D. Physical Review E 2001;63:1904.
[65] Helfer E, Harlepp S, Bourdieu L, Robert J, MacKintosh FC, Chatenay D. Physical Review Letters 2001;87(8) [Art. No. 088103].
[66] Ozkan M, Pisanic T, Scheel J, Barlow C, Esener S, Bhatia SN. Langmuir 2003;19(5):1532.
[67] Mills JP, Qie L, Dao M, Lim CT, Suresh S. Mechanics and Chemistry of Biosystems 2004;1:169.
[68] Sheetz MP. Laser tweezers in cell biology, vol. 55. San Diego: Academic Press; 1988.
[69] Guck J, Ananthakrishnan R, Cunningham CC, Kas J. Journal of Physics: Condensed Matter 2002;14(19):4843–56.
[70] Guck J, Ananthakrishnan R, Mahmood H, Moon TJ, Cunningham CC, Kas J. Biophysical Journal 2001;81(2):767–84.
[71] Guck J, Ananthakrishnan R, Moon TJ, Cunningham CC, Kas J. Physical Review Letters 2000;84(23):5451–4.
[72] Chang KS, Olbricht WL. Journal of Fluid Mechanics 1993;250: 609–33.
[73] Walter A, Rehage H, Leonhard H. Colloid and Polymer Science 2000; 278:169.
[74] Rehage H, Husmann M. Rheologica Acta 2002;41:292–306.
[75] Walter A, Rehage H, Leonhard H. Colloids and Surfaces A Physicochemical and Engineering Aspects 2001;183-185:123.
[76] Finken R, Seifert U. Journal of Physics: Condensed Matter 2006; 18(15):L185–91.
[77] Genzer J, Groenewold J. Soft Matter 2006;2:310–23.
[78] Pieper G, Rehage H, Barthes-Biesel D. Journal of Colloid and Interface Science 1998;202:293–300.
[79] Barthes-Biesel D. Flow-induced capsule deformation. Boca Raton: Chapman & Hall/CRC; 2003.
[80] Timoshenko S, Woinowsky-Krieger S. Theory of plates and shells, vol. xiv. New York: McGraw-Hill; 1959. 580 p.
[81] Ugural AC. Stresses in plates and shells, vol. xx. Boston, MA: WCB/McGraw Hill; 1999. 502 p.
[82] Niordson FI. Shell theory, vol. xiv. Amsterdam, New York, NY, North-Holland: Elsevier Science Pub Co.; 1985. Sole distributors for the U.S.A. and Canada, 408 p.
[83] Ramm E, Wall WA. International Journal for Numerical Methods in Engineering 2004;60(1):381–427.
[84] Helfrich W. Zeitschrift Naturforschung Section C 1973;28:693–703.

[85] Lipowsky R. Nature 1991;349(6309):475–81.
[86] Seifert U. Advances in Physics 1997;46(1):13–137.
[87] Gompper G, Kroll DM. Journal of Physics: Condensed Matter 1997;9(42):8795–834.
[88] Landau LD, Lifshitz EM. Theory of elasticity, vol. viii. Butterworth-Heinemann; 1986. 187 p.
[89] Koiter WT. A spherical shell under point loads at its poles. New York: Macmillan; 1963.
[90] Reissner E. Journal of Mathematics and Physics 1946;25:80.
[91] Reissner E. Journal of Mathematics and Physics 1946;25(4):279–300.
[92] Doghri I. Mechanics of deformable solids. Springer; 2000.
[93] Gregory RD, Milac TI, Wan FYM. SIAM Journal on Applied Mathematics 1999;59(3):1080–97.
[94] Lardner TJ, Pujara P. Compression of spherical cells; 1980.
[95] Liu KK, Williams DR, Briscoe BJ. Physical Review E 1996;54(6): 6673–80.
[96] Shilkrut D, Riks E. Stability of nonlinear shells: on the example of spherical shells, vol. xxi. New York: Elsevier Science Ltd; 2002. 458 p.
[97] Bushnell D. Computerized buckling analysis of shells, vol. xvii. Dordrecht; Boston Hingham, MA: Kluwer Academic; 1985. M. Nijhoff; [Distributors for the U.S. and Canada], 423 p.
[98] Kaplan A. Buckling of spherical shells. Prentice-Hall; 1974.
[99] Maccarini RR, Saetta A, Vitaliani R. Computer Methods in Applied Mechanics and Engineering 2001;190(37–38):4967–86.
[100] Lobkovsky A, Gentges S, Li H, Morse D, Witten TA. Science 1995;270(5241):1482–5.
[101] Pogorelov AV. Bendings of surfaces and stability of shells, vol. viii. Providence, R.I.: American Mathematical Society; 1988. 77 p.
[102] Taber LA. Journal of Applied Mechanics: Transactions of the ASME 1982;49(1):121–8.
[103] Zhongcan OY, Helfrich W. Physical Review A 1989;39(10): 5280–8.
[104] Boulbitch A. Journal of Electron Microscopy 2000;49(3):459–62.
[105] Wan KT, Chan V, Dillard DA. Colloids and Surfaces B: Biointerfaces 2003;27(2–3):241–8.
[106] Yao X, Walter J, Burke S, Stewart S, Jericho MH, Pink D, et al. Colloids and Surfaces B: Biointerfaces 2002;23(2–3):213–30.
[107] Arnoldi M, Fritz M, Bauerlein E, Radmacher M, Sackmann E, Boulbitch A. Physical Review E 2000;62(1):1034–44.
[108] Gao C, Donath E, Moya S, Dudnik V, Möhwald H. European Physical Journal E 2001;5:21–7.
[109] Quilliet C. Physical Review E 2006;74(4) [Art. No. 046608].
[110] Komura S, Tamura K, Kato T. European Physical Journal E 2005; 18(3):343–58.
[111] Schwarz US, Komura S, Safran SA. Europhysics Letters 2000; 50(6):762–8.
[112] Reddy JN. An introduction to the finite element method, vol. xvi. New York, NY: McGraw-Hill Higher Education; 2006. 766 p.
[113] Zienkiewicz OC, Taylor RL, Zhu JZ. The finite element method: its basis and fundamentals. Oxford; Burlington, MA: Elsevier/Butterworth-Heinemann; 2005.
[114] Zienkiewicz OC, Taylor RL. The finite element method for solid and structural mechanics, vol. xv. Oxford: Elsevier Butterworth-Heinemann; 2005. 631 p.
[115] Lim TJ, Smith B, McDowell DL. Acta Materialia 2002;50(11): 2867–79.
[116] Elsner N, Dubreuil F, Weinkamer R, Fischer FD, Wasicek F, Fery A. Progress in Colloid and Polymer Science 2006;132:117–32.
[117] Siber A. Physical Review E 2006;73(6):061915.
[118] Lidmar J, Mirny L, Nelson DR. Physical Review E 2003;68(5) [Art. No. 051910].
[119] Vliegenthart GA, Gompper G. Biophysics Journal 2006;91(3):834–41.
[120] Nguyen TT, Bruinsma RF, Gelbart WM. Physical Review E 2005;72(5) [Art. No. 051923].
[121] Linke GT, Lipowsky R, Gruhn T. Physical Review E 2005;71(5) [Art. No. 051602].
[122] Pauchard L, Rica S. Philosophical Magazine B: Physics of Condensed Matter Structural Electronic Optical and Magnetic Properties 1998; 78(2):225–33.
[123] Pauchard L, Pomeau Y, Rica S. Comptes Rendus de l Academie des Sciences Serie II Fascicule B-Mecanique Physique Chimie Astronomie 1997;324(7):411–8.
[124] Hutter JL, Bechhoefer J. Review of Scientific Instruments 1993; 64(7):1868.
[125] Sader JE, Chon JWM, Mulvaney P. Review of Scientific Instruments 1999;70(10):3967–9.
[126] Decher G. Science 1997;277(5330):1232–7.
[127] Decher G, Hong JD. Berichte Der Bunsen-Gesellschaft-Physical Chemistry Chemical Physics 1991;95(11):1430–4.
[128] Donath E, Sukhorukov GB, Caruso F, Davis SA, Möhwald H. Angewandte Chemie International Edition 1998;37(16):2202–5.
[129] Bäumler H, Artmann G, Voigt A, Mitlöhner R, Neu B, Kiesewetter H. Journal of Microencapsulation 2000;17(5):651–5.
[130] Gao C, Leporatti S, Moya S, Donath E, Möhwald H. Langmuir 2001;17:3491–5.
[131] Fery A, Dubreuil F, Möhwald H. New Journal of Physics 2004;6:18.
[132] Gingell D, Todd I. Biophysical Journal 1979;26(3):507–26.
[133] Rädler JO, Sackmann E. Journal of Physics II France 1993;3:727.
[134] Dubreuil F, Shchukin DG, Sukhorukov GB, Fery A. Macromolecular Rapid Communications 2004;25:1078.
[135] Heuvingh J, Zappa M, Fery A. Langmuir 2005;21(7):3165.
[136] Nolte AJ, Rubner MF, Cohen RE. Macromolecules 2005;38(13): 5367–70.
[137] Elsner N, Kozlovskaya V, Sukhishvili SA, Fery A. Soft Matter 2006; 2:966.
[138] Müller R, Köhler K, Weinkamer R, Sukhorukov GB, Fery A. Macromolecules 2005;38(23):9766–71.
[139] Delorme N, Fery A. Physical Review E 2006;74:030901.
[140] Daillant J, Bellet-Amalric E, Braslau A, Charitat T, Fragneto G, Graner F, et al. Proceedings of the National Academy of Sciences of the United States of America 2005;102:11639.
[141] Michel JP, Ivanovska IL, Gibbons MM, Klug WS, Knobler CM, Wuite GJL, et al. Proceedings of the National Academy of Sciences of the United States of America 2006;103(16):6184–9.
[142] Kol N, Gladnikoff M, Barlam D, Shnek RZ, Rein A, Rousso I. Biophysical Journal 2006;91(2):767–74.
[143] Delorme N, Dubois M, Garnier S, Laschewsky A, Weinkamer R, Zemb T, et al. Journal of Physical Chemistry B 2006;110:1752.
[144] de Pablo PJ, Schaap IAT, MacIntosh FC, Schmidt CF. Physical Review Letters 2003;91(9):098101.
[145] Graveland-Bikker JF, Schaap IAT, Schmidt CF, de Kruif CG. Nano Letters 2006;6(4):616–21.
[146] Kol N, Adler-Abramovic L, Barlam D, Shneck RZ, Gazit E, Rousso I. Nano Letters 2005;5(7):1343–6.
[147] Müller R, Daehne L, Fery A. Journal of Physical Chemistry B 2007;111:8547–53.
[148] Müller R, Daehne L, Fery A. Polymer 2007;48:2520–5.
[149] Cuenot S, Fretigny C, Demoustier-Champagne S, Nysten B. Physical Review B 2004;69:165410.
[150] Gao CY, Leporatti S, Moya S, Donath E, Mohwald H. Chemistry-A European Journal 2003;9(4):915–20.
[151] Dejugnat C, Sukhorukov G. Langmuir 2004;20:7265.
[152] Mauser T, Dejugnat C, Sukhorukov GB. Macromolecular Rapid Communications 2004;25:1781.
[153] Kozlovskaya V, Kharlampieva E, Sukhishvili SA. Chemistry of Materials 2006;18:328.
[154] Mauser T, Dejugnat C, Mohwald H, Sukhorukov GB. Langmuir 2006; 22:5888.
[155] Köhler K, Shchukin D, Möhwald H, Sukhorukov G. Journal of Physical Chemistry B 2005;109:18250.
[156] Biesheuvel PM, Mauser T, Sukhorukov G, Mohwald H. Macromolecules 2006;39:8480–6.
[157] Köhler K, Biesheuvel PM, Weinkamer R, Mohwald H, Sukhorukov G. Physical Review Letters 2006;97:188301.

Andreas Fery was born in Grieskirchen, Austria in 1972. He studied Physics at the University Konstanz, Germany and received his Ph.D. degree in Condensed Matter Physics in 2000 at the University of Potsdam, Germany/Max-Planck Institute of Colloids and Interfaces (MPIKG). After a Postdoc at the Institute Curie Paris, France in Biophysics he returned to the MPIKG as a group leader in 2001. In 2005 he was awarded the Richard Zsigmondy fellowship of the German colloid society. In 2007 he was appointed associate professor at the Physical Chemistry department of the University Bayreuth, Germany. His main research interests are interactions and nanomechanics of membranes, polymeric thin films and coatings as well as self assembly, surface patterning and force generation in biological systems.

Richard Weinkamer was born in Salzburg, Austria in 1967. He studied Physics at the University Vienna, Austria and received his Ph.D. degree in 2000 there in a joint project with the University of Rutgers, USA. After a Postdoc at the Erich Schmid Institute Leoben, Austria, he moved to the Max-Planck Institute of Colloids and Interfaces as a group leader in 2003. His main research interests are mechanobiological systems like bone, computer modelling of mechanics, growth and adaptation of biomaterials, structure–function relations and mechanical properties in biological tissues and phase transformation in natural and artificial materials.